

Segerstromite, $\text{Ca}_3(\text{As}^{5+}\text{O}_4)_2[\text{As}^{3+}(\text{OH})_3]_2$, the first mineral containing $\text{As}^{3+}(\text{OH})_3$, the arsenite molecule, from the Cobriza mine in the Atacama Region, Chile

HEXIONG YANG^{1,*}, ROBERT T. DOWNS¹, ROBERT A. JENKINS¹, AND STANLEY H. EVANS¹

¹Department of Geosciences, University of Arizona, Tucson, Arizona 85721-0077, U.S.A.

ABSTRACT

A new mineral species, segerstromite, ideally $\text{Ca}_3(\text{As}^{5+}\text{O}_4)_2[\text{As}^{3+}(\text{OH})_3]_2$, has been discovered at the Cobriza mine in the Sacramento district in the Copiapó Province, Chile. Crystals of segerstromite occur as tetrahedra, dodecahedra (up to $0.50 \times 0.50 \times 0.50$ mm), or in blocky aggregates. Associated minerals include talmessite, vladimirite, and Sr-bearing hydroxylapatite. Similar to the associated minerals, segerstromite is a secondary mineral. The new mineral is colorless in transmitted light, transparent with a white streak and vitreous luster. It is brittle and has a Mohs hardness of ~4.5. No cleavage, parting, or twinning was observed. The measured and calculated densities are 3.44(3) and 3.46 g/cm³, respectively. Optically, segerstromite is isotropic, with $n = 1.731(5)$. It is insoluble in water or hydrochloric acid. An electron microprobe analysis yielded an empirical formula (based on 14 O apfu) $\text{Ca}_{2.98}(\text{AsO}_4)_{2.00}[\text{As}(\text{OH})_3]_{2.00}$.

Segerstromite is cubic, with space group $I2_13$ and unit-cell parameters $a = 10.7627(2)$ Å, $V = 1246.71(4)$ Å³, and $Z = 4$. Its crystal structure is constructed from three different polyhedral units: distorted CaO_8 cubes, rigid As^{5+}O_4 arsenate tetrahedra, and neutral $\text{As}^{3+}(\text{OH})_3$ arsenite triangular pyramids. The Ca-groups form layers of corrugated crankshaft chains that lie parallel to the cubic axes. These chains are linked by the isolated As^{5+}O_4 and $\text{As}^{3+}(\text{OH})_3$ groups. Segerstromite is the first known crystalline compound that contains the $\text{As}^{3+}(\text{OH})_3$ arsenite molecule, pointing to a new potential approach to remove highly toxic and mobile $\text{As}^{3+}(\text{OH})_3$ from drinking water.

Keywords: New mineral, segerstromite, arsenate/arsenite, crystal structure, X-ray diffraction, Raman spectrum

INTRODUCTION

A new mineral species, segerstromite, ideally $\text{Ca}_3(\text{As}^{5+}\text{O}_4)_2[\text{As}^{3+}(\text{OH})_3]_2$, has been found at the Cobriza mine in the Sacramento district in the Copiapó Province, Atacama Region, Chile. It is named in honor of the late Kenneth Segerstrom (1909–1992), who was a professional geologist and worked more than 40 yr for the U.S. Geological Survey in the U.S., Mexico, and Chile, principally conducting field-based regional geologic studies. In particular, Ken Segerstrom worked in Chile in conjunction with the “Instituto de Investigaciones Geológicas” (now Sernageomin), from 1957–1963, mainly in the Atacama Region, where the new mineral was found. Among his numerous publications, Ken Segerstrom authored 18 maps and articles on the Atacama Region, including the Sacramento district and the Cobriza mine. The new mineral and its name have been approved by the Commission on New Minerals, Nomenclature and Classification (CNMNC) of the International Mineralogical Association (IMA 2014-001). Part of the co-type sample has been deposited at the University of Arizona Mineral Museum (catalog no. 19800) and the RRUFF Project (deposition no. R130753).

Arsenic contamination can be a major ecological hazard because of its well-known toxicity and carcinogenicity, even at very low concentrations in drinking water (10 µg/L) (Hughes 2002; Vaughan 2011). In natural water, arsenic primarily exists in

inorganic forms with two predominant species: $\text{H}_3\text{As}^{3+}\text{O}_3$ arsenite [or commonly written as $\text{As}^{3+}(\text{OH})_3$] and $\text{H}_3\text{As}^{5+}\text{O}_4$ arsenate. The toxicity of arsenic depends strongly on its oxidation state, with As^{3+} 25–60 times more toxic than As^{5+} (Fazal et al. 2001). Although some sophisticated methods have been developed to remove As^{5+} from drinking water, such as by ion-exchange, adsorption, or as a precipitate of AlAsO_4 or FeAsO_4 , there is no efficient or economic approach to eliminate As^{3+} as yet, due partly to its greater solubility and mobility than As^{5+} (e.g., Zhang et al. 2007; Mohan and Pittman 2007; Itakura et al. 2008; Kreidie et al. 2011; Roy et al. 2016; Dickson et al. 2017; Yadav et al. 2017). Extensive efforts, both experimental and theoretical, have been devoted to seeking ligands that can form stable complexes with $\text{As}^{3+}(\text{OH})_3$ and some successes have been achieved with certain organic compounds (e.g., Porquet and Filella 2007; Kolozsi et al. 2008). Nonetheless, there has been no report for the presence of the $\text{As}^{3+}(\text{OH})_3$ group in any inorganic crystalline material, synthetic or natural, until now. Therefore, segerstromite represents the first inorganic compound that sequesters the $\text{As}^{3+}(\text{OH})_3$ group in its structure.

SAMPLE DESCRIPTION AND EXPERIMENTAL METHODS

Occurrence, physical and chemical properties, and Raman spectra

Segerstromite was found on several specimens collected by R.A.J. from the Cobriza mine (27°49'45"S, 70°14'03"W) in the Sacramento district in the Copiapó Province, Atacama Region, Chile. The Cobriza mine is an abandoned Pb-Ag-

* E-mail: hyang@email.arizona.edu

As-Cu-Zn mine; the mineralization is hosted in sedimentary and volcanic rocks.

Crystals of segerstromite occur as tetrahedra, dodecahedra, granular or blocky aggregates, with single crystals up to $0.50 \times 0.50 \times 0.50$ mm (Fig. 1). Associated minerals include talmezzite $\text{Ca}_2\text{Mg}(\text{AsO}_4)_2 \cdot 2\text{H}_2\text{O}$, vladimirite $\text{Ca}_4(\text{AsO}_4)_2(\text{AsO}_3\text{OH}) \cdot 4\text{H}_2\text{O}$, and Sr-bearing hydroxylapatite $\text{Ca}_4(\text{PO}_4)_3(\text{OH})$. Similar to the other associated minerals (talmezzite and vladimirite), segerstromite is considered to be a secondary mineral. Vladimirite from the Cobriza mine has been previously investigated by Yang et al. (2011).

Segerstromite is colorless in transmitted light, transparent with a white streak and vitreous luster. It is brittle and has a Mohs hardness of ~4.5; no cleavage, parting, or twinning was observed. The measured (by flotation) and calculated densities are 3.44(3) and 3.46 g/cm³, respectively. Optically, segerstromite is isotropic, with $n = 1.731(5)$, measured in white light. It is insoluble in water or hydrochloric acid.

The chemical composition of segerstromite was determined using a CAMECA SX-100 electron microprobe (WDS mode, 10 kV, 6 nA, and 10 μm beam diameter). The standards included As_2O_3 for As, and wollastonite (CaSiO_3) for Ca, yielding an average composition (wt%) (16 points) of As_2O_3 60.75(16) [converted to As_2O_3 30.38 + As_2O_5 35.20 with $\text{As}^{3+}/\text{As}^{5+} = 1$ according to the X-ray structure determination, see below], CaO 25.57(12), H_2O 8.29 (added according to the structure determination), and total = 99.53(26). The resultant chemical formula, calculated on the basis of 14 O apfu (from the structure determination), is $\text{Ca}_{2.98}(\text{AsO}_4)_{2.00}[\text{As}(\text{OH})_3]_{2.00}$, which can be simplified to $\text{Ca}_3(\text{As}^{5+}\text{O}_4)_2[\text{As}^{3+}(\text{OH})_3]_2$.

The Raman spectrum of segerstromite was collected on a randomly oriented crystal on a Thermo-Almega microRaman system, using a solid-state laser with

a frequency of 532 nm and a thermoelectric cooled CCD detector. The laser is partially polarized with 4 cm⁻¹ resolution and a spot size of 1 μm .

X-ray crystallography

Both the powder and single-crystal X-ray diffraction data for segerstromite were collected on a Bruker X8 APEX2 CCD X-ray diffractometer equipped with graphite-monochromatized $\text{MoK}\alpha$ radiation. Table 1 lists the measured powder X-ray diffraction data, along with those calculated from the determined structure using the program XPOW (Downs et al. 1993).

Single-crystal X-ray diffraction data of segerstromite were collected from a nearly equidimensional crystal ($0.05 \times 0.04 \times 0.04$ mm) with frame widths of 0.5° in ω and 30 s counting time per frame. All reflections were indexed on the basis of a cubic unit cell (Supplemental¹ Table 1). The intensity data were corrected for X-ray absorption using the Bruker program SADABS. The systematic absences of reflections suggest possible space group $I23$, $I2_13$, or $Im\bar{3}$. The crystal structure was solved and refined using SHELX2014 (Sheldrick 2015a, 2015b) based on space group $I2_13$, because it produced the better refinement statistics in terms of bond lengths and angles, atomic displacement parameters, and R factors. The H atom was located from the difference Fourier maps. The ideal chemistry was assumed during the refinements. The positions of all atoms were refined with anisotropic displacement parameters, except those for the H atom, which was refined with an isotropic parameter. Final coordinates and displacement parameters of atoms in segerstromite are listed in Table 2, and selected bond distances in Supplemental¹ Table 2. Calculated bond-valence sums using the parameters from Brese and O'Keeffe (1991) are given in Table 3.

DISCUSSION

Crystal structure

The crystal structure of segerstromite is unique. It is constructed from three different polyhedral units: distorted CaO_8 cubes with six short and two long Ca-O bonds, rigid As^{5+}O_4 arsenate tetrahedra, and neutral $\text{As}^{3+}(\text{OH})_3$ arsenite triangular pyramids (Table 2 and Fig. 2). The As^{5+}O_4 and $\text{As}^{3+}(\text{OH})_3$ groups are isolated from each other, while the Ca-groups form corrugated crankshaft chains that layer perpendicular to the cubic axes (Fig. 3). The corrugations are stabilized by the $\text{As}^{3+}(\text{OH})_3$ arsenite groups. The layers are stacked with a shift



FIGURE 1. (a) Rock samples on which segerstromite crystals are found. (b) A microscopic view of segerstromite showing the tetrahedral morphology. (Color online.)

TABLE 1. Powder diffraction data for segerstromite

Intensity	Experimental		Theoretical			
	<i>d</i> -spacing	<i>d</i> -spacing	<i>d</i> -spacing	<i>h</i>	<i>k</i>	<i>l</i>
34	4.351	8.52	4.3939	2	1	1
25	3.775	28.74	3.8052	2	2	0
82	3.389	77.54	3.4035	3	0	1
		22.46	3.4035	3	1	0
33	3.104	39.94	3.1069	2	2	2
100	2.875	16.47	2.8765	3	2	1
		77.46	2.8765	3	1	2
7	2.691	27.58	2.6907	4	0	0
14	2.536	13.93	2.5368	4	1	1
		7.08	2.2946	3	3	2
		27.77	2.1969	4	2	2
		5.24	2.1107	4	3	1
45	2.111	32.87	2.1107	5	1	0
7	1.965	8.86	1.9650	5	2	1
27	1.905	44.44	1.9026	4	4	0
34	1.748	8.16	1.7459	5	3	2
		17.10	1.7459	6	1	1
		4.84	1.7459	5	2	3
11	1.703	10.50	1.7017	6	2	0
		14.73	1.7017	6	0	2
16	1.663	8.67	1.6607	5	4	1
7	1.624	5.00	1.6225	6	2	2
13	1.588	3.39	1.5869	6	3	1
		12.25	1.5869	6	1	3
12	1.524	4.84	1.5221	5	3	4
19	1.465	8.63	1.4646	7	1	2
		9.08	1.4646	7	2	1
		3.05	1.4646	6	3	3

of half a unit cell, so that the chains lie above and below the gaps between the chains (Fig. 4). The corrugated layers are held together by chains of CaO₈ groups linked by the isolated AsO₄ arsenate groups (Fig. 5).

There are several minerals that contain both As⁵⁺ and As³⁺ (Table 4), but segerstromite is the first known crystalline compound that contains the neutral As³⁺(OH)₃ arsenite group. The average As³⁺-O bond length for the As³⁺(OH)₃ group is 1.776 Å, in excellent agreement with the experimental value of 1.77–1.78 Å reported for the As³⁺(OH)₃ molecule in aqueous solutions (Arai et al. 2001; Pokrovski et al. 2002; Ramirez-Solis et al. 2004; Testamale et al. 2004). It also falls in the range between 1.77 and 1.82 Å calculated by various

theoretical methods (see Porquet and Filella 2007; Tossell and Zimmermann 2008; Hernández-Cobos et al. 2010). The O-As³⁺-O angle is 95.29°, with a trigonal pyramidal lone-pair-As³⁺-O angle of 121.43°.

The As⁵⁺O₄ tetrahedron is slightly distorted, with the As1-O1 bond length (1.698 Å) longer than the three As1-O2 distances (1.679 Å) (Table 2). The average As⁵⁺-O bond length is 1.684 Å, in accord with the values found in many other arsenate minerals (Hawthorne et al. 2012; Kampf et al. 2015; Đorđević et al. 2016 and references therein), as well as the average value of 1.685 Å derived by Majzlan et al. (2014) through an examina-

TABLE 2. Selected bond distances and angles in segerstromite

As1-O1 (Å)	1.698(2)
As1-O2	1.679(1) ×3
Avg.	1.684
As2-O3 (Å)	1.776(1) ×3
Ca-O1 (Å)	2.430(1) ×2
Ca-O2	2.381(1) ×2
Ca-O2	2.932(1) ×2
Ca-O3	2.448(1) ×2
Avg.	2.548
O3-H...O2 (Å)	2.664(2)
O3-H (Å)	0.78(2)
∠O3-H...O2 (°)	177(2)

Note: Coordinates and displacement parameters of atoms in segerstromite.

TABLE 3. Calculated bond-valence sums for segerstromite

	O1	O2	O3	Sum
Ca	0.286 ×2	0.327 ×2 0.074 ×2	0.272 ×2→	1.918
As1	1.279	1.345 ×3→		5.161
As2			1.035 ×3→	3.104
Sum	1.851	2.146	1.307	

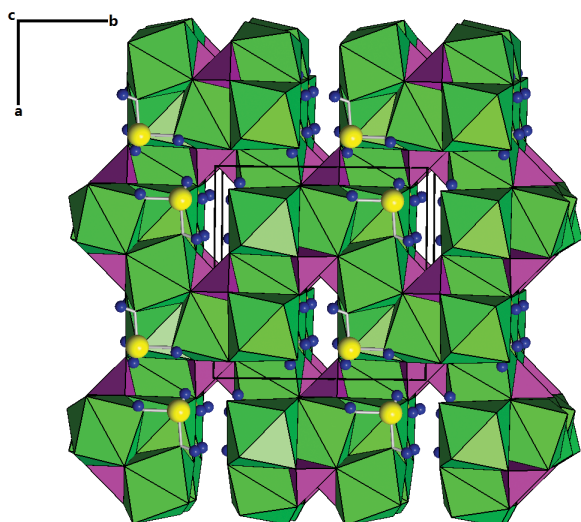


FIGURE 2. Crystal structure of segerstromite. The green and purple polyhedra represent CaO₈ and As⁵⁺O₄ groups, respectively. The large yellow and small blue spheres represent As³⁺ (As2) and H atoms, respectively. (Color online.)

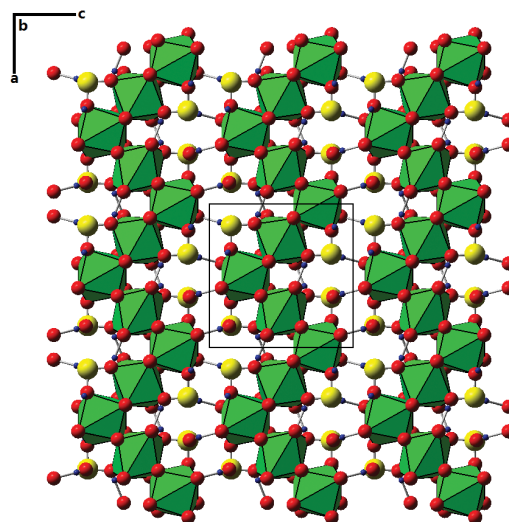


FIGURE 3. A slice of the segerstromite structure, showing corrugated crankshaft chains formed by the corner-shared, distorted CaO₈ cubes. The corrugations are stabilized by the As³⁺(OH)₃ arsenite groups. The green polyhedra represent the distorted CaO₈ cubes. The large yellow, medium red, and small blue spheres represent As³⁺, O, and H atoms, respectively. (Color online.)

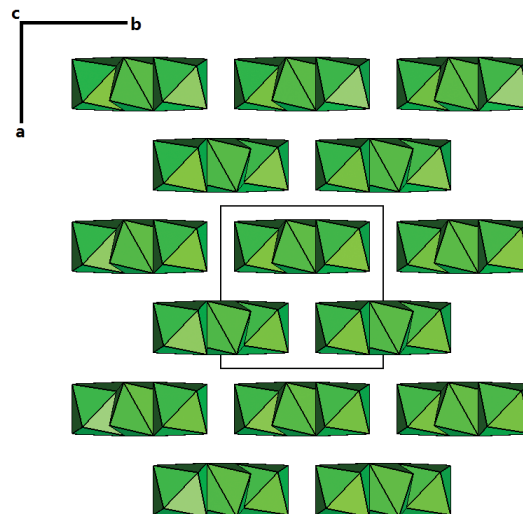


FIGURE 4. The segerstromite structure showing the layers formed by the corrugated chains of the corner-shared CaO₈ cubes. (Color online.)

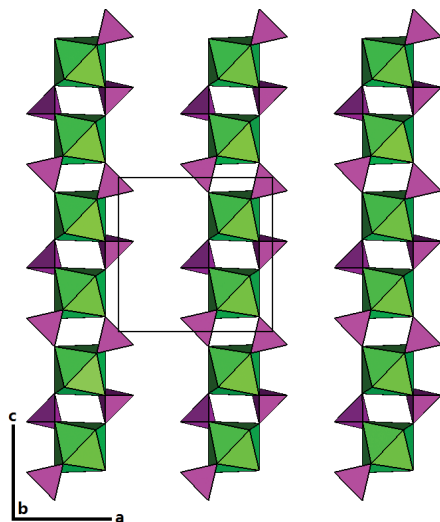


FIGURE 5. The segerstromite structure showing chains of CaO_6 groups linked by the isolated AsO_4 arsenate groups. (Color online.)

TABLE 4. Minerals containing both As^{5+} and As^{3+} as essential components

Mineral name	Chemical formula
Segerstromite	$\text{Ca}_5(\text{AsO}_4)_2[\text{As}(\text{OH})_3]_2$
Arakiite	$\text{Zn}^{2+}\text{Mn}_2^{2+}\text{Fe}_2^{3+}(\text{As}^{5+}\text{O}_3)(\text{As}^{5+}\text{O}_4)_2(\text{OH})_{23}$
Carlfrancisite	$\text{Mn}_3^{2+}(\text{Mn}^{2+}, \text{Mg}, \text{Fe}^{3+}, \text{Al})_{42}[\text{As}^{3+}\text{O}_3]_2(\text{As}^{5+}\text{O}_4)_4$ $[(\text{Si}, \text{As}^{5+})\text{O}_4]_6[(\text{As}^{5+}, \text{Si})\text{O}_4]_2(\text{OH})_{42}$
Dixenite	$\text{Cu}^{1+}\text{Mn}_2^{2+}\text{Fe}_2^{3+}(\text{As}^{5+}\text{O}_3)_5(\text{SiO}_4)_2(\text{As}^{5+}\text{O}_4)(\text{OH})_6$
Hematolite	$(\text{Mn}^{2+}, \text{Mg}, \text{Al})_{15}(\text{As}^{3+}\text{O}_3)(\text{As}^{5+}\text{O}_4)_2(\text{OH})_{23}$
McGovernite	$\text{Mn}_2^{2+}\text{Zn}_2^{2+}(\text{As}^{3+}\text{O}_3)(\text{As}^{5+}\text{O}_4)_3(\text{SiO}_4)_3(\text{OH})_{21}$
Radovanite	$\text{Cu}_2^{2+}\text{Fe}^{3+}(\text{As}^{3+}\text{O}_3)(\text{OH})_2(\text{As}^{5+}\text{O}_4)_2 \cdot \text{H}_2\text{O}$
Synadelphite	$\text{Mn}_3^{2+}(\text{As}^{3+}\text{O}_3)(\text{As}^{5+}\text{O}_4)_2(\text{OH})_9 \cdot 2\text{H}_2\text{O}$
Vicanite-(Ce)	$(\text{Ca}, \text{Ce}, \text{La}, \text{Th})_{15}\text{As}^{5+}(\text{As}^{3+}, \text{Na})_{0.5}\text{Fe}_{0.7}^{3+}\text{Si}_6\text{B}_4(\text{O}, \text{F})_{47}$

TABLE 5. Tentative assignments of major Raman bands for segerstromite

Bands (cm^{-1})	Assignment
2906	O-H stretching vibration
2449	Stretching vibration of the strongly hydrogen-bonded OH in the $\text{As}(\text{OH})_3$ unit (Frost et al. 2011)
790–910	As^{5+} -O stretching vibrations within the AsO_4 group
610–750	As^{3+} -O stretching vibrations within the $\text{As}(\text{OH})_3$ groups
300–500	O- As^{5+} -O and O- As^{3+} -O bending vibrations within AsO_4 and $\text{As}(\text{OH})_3$ groups
<300	Lattice and Ca-O vibrational modes

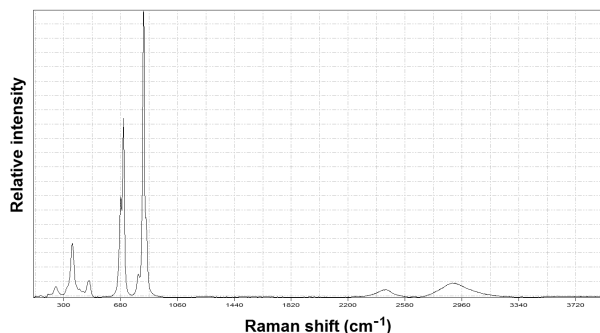


FIGURE 6. Raman spectra of segerstromite.

tion of numerous arsenate minerals.

The hydrogen-bonding scheme in segerstromite is presented in Table 2. The $\text{O}_3\text{-H}\cdots\text{O}_2$ distance is 2.664(2) Å, indicating a considerably strong hydrogen bond.

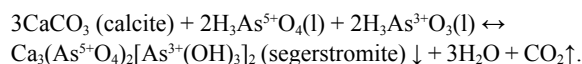
Raman spectrum

Numerous Raman spectroscopic studies have been conducted on various arsenite and/or arsenate minerals and compounds (e.g., Frost et al. 2011; Kharbush 2012; Liu et al. 2014; Đorđević 2015; Đorđević et al. 2016, and references therein), as well as on the $\text{As}(\text{OH})_3$ molecule in organic materials and solutions (e.g., Loehr and Plane 1968; Pokrovski et al. 1999; Goldberg and Johnston 2001; Wood et al. 2002; Müller et al. 2010). The Raman spectrum of segerstromite is displayed in Figure 6 and the tentative assignments of major Raman bands based on the previous studies are given in Table 5. In particular, the bands at 699 and 680 cm^{-1} are ascribed to the symmetric and asymmetric stretching vibrations of As-OH within the $\text{As}^{3+}(\text{OH})_3$ group, respectively, which should be compared with 701–710 and 655–669 cm^{-1} observed for the $\text{As}(\text{OH})_3$ group in aqueous solutions (Loehr and Plane 1968; Pokrovski et al. 1999; Goldberg and Johnston 2001; Müller et al. 2010).

In Figure 6, the O-H stretching vibration is marked by a broad band at 2906 cm^{-1} . According to Libowitzky (1999), an $\text{O-H}\cdots\text{O}$ distance of 2.66 Å would correspond to an O-H stretching frequency of $\sim 2900 \text{ cm}^{-1}$, consistent with our measured value. Similar results were also reported for diaspore, which has an O-H \cdots O distance of 2.65 Å with the O-H \cdots O angle of 160.8° (Hill 1979) and a Raman band at 2918 cm^{-1} that is attributable to the O-H stretching vibration (Ruan et al. 2001).

IMPLICATIONS

In comparison to As^{5+} , besides its greater toxicity, $\text{As}^{3+}(\text{OH})_3$ is also more mobile and soluble in the environment because of its neutral character in a wide pH range (<9.2 at 25 °C with $\text{As} = 0.1 \text{ mol/L}$) (Müller et al. 2010), resulting in its weaker adsorption on soil constituents, such as iron and aluminum oxy-hydroxides (Ladeira and Ciminelli 2004; Yokoyama et al. 2012). All previous investigations have appeared to focus chiefly on the understanding of how $\text{As}^{3+}(\text{OH})_3$ can be immobilized with the formation of complexes with Fe^{3+} and Al^{3+} . In particular, the possibility of co-precipitation of As^{3+} and Fe^{3+} has been explored extensively, because such a phenomenon has been observed to take place in natural environments, as well as under laboratory conditions (e.g., Ciardelli et al. 2008; Sasaki et al. 2009; Müller et al. 2010). Recently, Itakura et al. (2007, 2008) proposed the removal of arsenic from water containing both arsenite and arsenate ions through the hydrothermal formation of the mineral johnbaumite, $\text{Ca}_5(\text{As}^{5+}\text{O}_4)_3(\text{OH})$ (arsenate analog of apatite). The discovery of segerstromite, however, points to a new potential approach to remove or reduce $\text{As}^{3+}(\text{OH})_3$ in water, providing sufficient availability of Ca^{2+} . Because calcite, CaCO_3 , is the most stable polymorph of calcium carbonates under the ambient conditions and ubiquitously found in various surface environments, a potential chemical reaction for such a process would be:



Hence, further investigations on the formation conditions of segerstromite, such as pH, Eh, and temperature, will undoubtedly generate information on how to remove $\text{As}^{3+}(\text{OH})_3$ in water more efficiently and economically.

ACKNOWLEDGMENTS

This study was funded by the Science Foundation Arizona. The constructive comments by Anthony R. Kampf and an anonymous reviewer are greatly appreciated.

REFERENCES CITED

- Arai, Y., Elzinga, E.J., and Sparks, D. (2001) X-ray absorption spectroscopic investigation of arsenite and arsenate adsorption at the aluminum oxide-water interface. *Journal of Colloid and Interfacial Science*, 235, 80–88.
- Brese, N.E., and O'Keeffe, M. (1991) Bond-valence parameters for solids. *Acta Crystallographica*, B47, 192–197.
- Ciardelli, M.C., Xu, H., and Sahai, N. (2008) Role of Fe(II), phosphate, silicate, sulfate, and carbonate in arsenic uptake by coprecipitation in synthetic and natural groundwater. *Water Research*, 42, 615–624.
- Dickson, D., Liu, G., and Cai, Y. (2017) Adsorption kinetics and isotherms of arsenite and arsenate on hematite nanoparticles and aggregates. *Journal of Environmental Management*, 186, 261–267.
- Dorđević, T. (2015) Crystal chemistry of the $M1^{1+2+}$ - $M2^{2+3+}$ -H-arsenites: the first cadmium(II) arsenite, $\text{Na}_4\text{Cd}(\text{AsO}_3)_6$. *Zeitschrift für Anorganische und Allgemeine Chemie*, 641, 1863–1868.
- Dorđević, T., Kolitsch, U., and Nasadala, L. (2016) A single-crystal X-ray and Raman spectroscopic study of hydrothermally synthesized arsenates and vanadates with the descloizite and adelite structure types. *American Mineralogist*, 101, 1135–1149.
- Downs, R.T., Bartelmebs, K.L., Gibbs, G.V., and Boisen, M.B. Jr. (1993) Interactive software for calculating and displaying X-ray or neutron powder diffractometer patterns of crystalline materials. *American Mineralogist*, 78, 1104–1107.
- Fazal, M. A., Kawachi, T., and Ichion, E. (2001) Extent and severity of ground-water arsenic contamination in Bangladesh. *Water International*, 26, 370–379.
- Frost, R.L., Čejka, J., Sejkora, J., Plášil, J., Bahfenne, S., and Keeffe, E.C. (2011) Raman spectroscopy of hydrogen arsenate group (AsO_3OH)₂ in solid-state compounds: cobalt-containing zinc arsenate mineral, koritnigite (Zn,Co) (AsO_3OH)₂·H₂O. *Journal of Raman Spectroscopy*, 42, 534–539.
- Goldberg, S., and Johnston, C.T. (2001) Mechanisms of arsenic adsorption on amorphous oxides evaluated using macroscopic measurements, vibrational spectroscopy, and surface complexation modeling. *Journal of Colloid and Interfacial Science*, 234, 204–216.
- Hawthorne, F.C., Cooper, M.A., Abdu, Y.A., Ball, N.A., Back, M.E., and Tait, K.T. (2012) Davidlloydite, ideally $\text{Zn}_3(\text{AsO}_4)_2(\text{H}_2\text{O})_4$, a new arsenate mineral from the Tsumeb mine, Otjikoto (Oshikoto) region, Namibia: description and crystal structure. *Mineralogical Magazine*, 76, 45–57.
- Hernández-Cobos, J., Cristina Vargas, M., Ramirez-Solis, A. and Ortega-Blake, I. (2010) Aqueous solvation of $\text{As}(\text{OH})_3$: A Monte Carlo study with flexible polarizable classical interaction potentials. *The Journal of Chemical Physics*, 133, 114501.
- Hill, R.J. (1979) Crystal structure refinement and electron density distribution in diaspore. *Physics and Chemistry of Minerals*, 5, 179–200.
- Hughes, M.F. (2002) Arsenic toxicity and potential mechanisms of action. *Toxicology Letter*, 133, 1–16.
- Itakura, T., Sasai, R., and Itoh, H. (2007) Arsenic recovery from water containing arsenite and arsenate ions by hydrothermal mineralization. *Journal of Hazardous Materials*, 328–333.
- (2008) A precipitation method for arsenite ion in aqueous solution as natural mineral by hydrothermal mineralization. *Journal of the Ceramic Society of Japan*, 116, 234–238.
- Kampf, A.R., Mills, S.J., Nash, B.P., Dini, M., and Donoso, A.A.M. (2015) Tapiaitite, $\text{Ca}_5\text{Al}_2(\text{AsO}_4)_6(\text{OH})_4 \cdot 12\text{H}_2\text{O}$, a new mineral from the Jote mine, Tierra Amarilla, Chile. *Mineralogical Magazine*, 79, 345–354.
- Kharbish, S. (2012) Raman spectra of minerals containing interconnected $\text{As}(\text{Sb})\text{O}_3$ pyramids: trippkeite and schafarzikite. *Journal of Geosciences*, 57, 53–62.
- Kolozsi, A., Lakatos, A., Galbács, G., Madsen, A.Ø., Larsen, E., and Gyurcsik, B. (2008) A pH-Metric, UV, NMR, and X-ray crystallographic study on arsenous acid reacting with dithioerythritol. *Inorganic Chemistry*, 47, 3832–3840.
- Kreidie, N., Armiesto, G., Cibin, G., Cinque, G., Crovato, C., Nardi, E., Pacifico, R., Cremisini, C., and Mottana, A. (2011) An integrated geochemical and mineralogical approach for the evaluation of arsenic mobility in mining soils. *Journal of Soils and Sediments*, 11, 37–52.
- Ladeira, A.C.Q., and Ciminelli, V.S.T. (2004) Adsorption and desorption of arsenic on an oxisol and its constituents. *Water Research*, 38, 2087–2094.
- Libowitzky, E. (1999) Correlation of O-H stretching frequencies and O-H···O hydrogen bond lengths in minerals. *Monatshhefte für Chemie*, 130, 1047–1059.
- Liu, J., Jia, R., and Liu, J. (2014) The vibration characterization of synthetic crystalline lead hydrogen arsenite chloride precipitates $\text{Pb}_2(\text{HAsO}_3)_2\text{Cl}_2$ —implications of solidification of As (III) and Pb (II). *Spectrochimica Acta Part A: Molecular and Biomolecular Spectroscopy*, 117, 658–661.
- Loehr, T.M., and Plane, R.A. (1968) Raman spectra and structures of arsenious acid and arsenites in aqueous solution. *Inorganic Chemistry*, 7, 1708–1714.
- Majzlan, J., Drahotka, P., and Filippi, M. (2014) Parageneses and crystal chemistry of arsenic minerals. *Reviews in Mineralogy and Geochemistry*, 79, 17–184.
- Mohan, D., and Pittman, C.U. Jr. (2007) Arsenic removal from water/wastewater using adsorbents—A critical review. *Journal of Hazardous Materials*, 142, 1–53.
- Müller, K., Ciminelli, V.S.T., Dantas, M.S.S., and Willscher, S. (2010) A comparative study of As(III) and As(V) in aqueous solutions and adsorbed on iron oxy-hydroxides by Raman spectroscopy. *Water Research*, 44, 5660–5672.
- Pokrovski, G.D., Bény, J.-M., and Zotov, A. (1999) Solubility and Raman spectroscopic study of As(III) speciation in organic compound-water solutions. A hydration approach for aqueous arsenic in complex solutions. *Journal of Solution Chemistry*, 28, 1307–1327.
- Pokrovski, G.S., Zakirov, I., Roux, J., Testemale, D., Hazemann, J.-L., Bychkov, A. Yu., and Golikova, G.V. (2002) Experimental study of arsenic speciation in vapor phase to 500 °C: implications for As transport and fractionation in low-density crustal fluids and volcanic gases. *Geochimica et Cosmochimica Acta*, 66, 3453–3480.
- Porquet, A., and Filella, M. (2007) Structural evidence of the similarity of $\text{Sb}(\text{OH})_3$ and $\text{As}(\text{OH})_3$ with glycerol: Implications for their uptake. *Chemical Research of Toxicology*, 20, 1269–1276.
- Ramirez-Solis, A., Mukopadhyay, R., Rosen, B.P., and Stemmler, T.L. (2004) Experimental and theoretical characterization of arsenite in water: insights into the coordination environment of As-O. *Inorganic Chemistry*, 43, 2954–2959.
- Roy, E., Patra, S., Rashmi Madhuri, R., and Sharma, P.K. (2016) A single solution for arsenite and arsenate removal from drinking water using cysteine@ZnS:TiO₂ nanoparticle modified molecularly imprinted biofouling-resistant filtration membrane. *Chemical Engineering Journal*, 304, 259–270.
- Ruan, H.D., Frost, R.L., and Klopogge, J.T. (2001) Comparison of Raman spectra in characterizing gibbsite, bayerite, diaspore and boehmite. *Journal of Raman Spectroscopy*, 32, 745–750.
- Sasaki, K., Nakano, H., Wilopo, W., Miura, Y., and Hirajima, T. (2009) Sorption and speciation of arsenic by zero-valent iron. *Colloids and Surfaces A: Physicochemical Engineering Aspects*, 347, 8–17.
- Sheldrick, G.M. (2015a) SHELXT—Integrated space-group and crystal structure determination. *Acta Crystallographica*, A71, 3–8.
- (2015b) Crystal structure refinement with SHELX. *Acta Crystallographica*, C71, 3–8.
- Testemale, D., Hazemann, J.-L., Pokrovski, G.S., Joly, Y., Roux, J., Argoud, R., and Geaymond, O. (2004) Structural and electronic evolution of the $\text{As}(\text{OH})_3$ molecule in high temperature aqueous solutions: an X-ray absorption investigation. *Journal of Chemical Physics*, 121, 8973–8982.
- Tossell, J.A., and Zimmermann, M.D. (2008) Calculation of the structures, stabilities, and vibrational spectra of arsenites, thioarsenites and thioarsenates in aqueous solution. *Geochimica et Cosmochimica Acta*, 72, 5232–5242.
- Vaughan, D.J. (2011) Arsenic. *Elements*, 2, 71–75.
- Wood, S.A., Tait, C.D., and Janecky, D.R. (2002) A Raman spectroscopic study of arsenite and thioarsenite species in aqueous solution at 25 °C. *Geochemical Transactions*, 3, 31–39.
- Yadav, M.K., Gupta, A.K., Ghosal, P.S., and Mukherjee, A. (2017) pH mediated facile preparation of hydrotalcite based adsorbent for enhanced arsenite and arsenate removal: Insights on physicochemical properties and adsorption mechanism. *Journal of Molecular Liquids*, 240, 240–252.
- Yang, H., Evans, S.H., Downs, R.T., and Jenkins, R.A. (2011) The crystal structure of vladimirite, with a revised chemical formula, $\text{Ca}_4(\text{AsO}_4)_2(\text{AsO}_3\text{OH}) \cdot 4\text{H}_2\text{O}$. *Canadian Mineralogist*, 49, 1055–1064.
- Yokoyama, Y., Kazuya Tanaka, K., and Takahashi, Y. (2012) Differences in the immobilization of arsenite and arsenate by calcite. *Geochimica et Cosmochimica Acta*, 91, 202–219.
- Zhang, G., Qu, J., Liu, H., Liu, R., and Li, G. (2007) Removal mechanism of As(III) by a novel Fe-Mn binary oxide adsorbent: Oxidation and sorption. *Environmental Science & Technology*, 41, 4613–4619.

MANUSCRIPT RECEIVED OCTOBER 12, 2017

MANUSCRIPT ACCEPTED MAY 11, 2018

MANUSCRIPT HANDLED BY G. DIEGO GATTA

Endnote:

¹Deposit item AM-18-96329, Supplementary Tables and CIF. Deposit items are free to all readers and found on the MSA web site, via the specific issue's Table of Contents (go to http://www.minsocam.org/MSA/AmMin/TOC/2018/Sep2018_data/Sep2018_data.html).